Cell and organ transplantology
SCIENTIFIC JOURNAL
КЛІТИННА ТА ОРГАННА ТРАНСПЛАНТОЛОГІЯ | КЛІТИННА ТА ОРГАННА ТРАНСПЛАНТОЛОГІЯ

ORIGINAL RESEARCH
Cell and Organ Transplantology. 2024; 13(1):in press (e2025131177)
https://doi.org/10.22494/cot.v13i1.177

Granulocyte colony-stimulating factor modulates glial scar formation after hemorrhagic stroke in rats by mobilizing mesenchymal cells

Grabovoy A., Mervinsky T., Savosko S., Kondaurova H., Konovalova L., Yaremenko L.
Bogomolets National Medical University, Kyiv, Ukraine
Corresponding author's e-mail: xabalas1@gmail.com

Abstract

A glial scar typically develops in the brain following a stroke and represents a common astrocytic response to injury. While astrocytes are the primary cell type involved in this process, non-glial cells also contribute to scar formation. The immunophenotype of these additional cell populations remains poorly characterized. Identifying these cells could deepen our understanding of glial scar development and help uncover potential therapeutic targets.

Aim. *To identify cells of potential mesenchymal origin in the glial scar following hemorrhagic stroke (HS) and assess changes in their number under the influence of granulocyte colony-stimulating factor (G-CSF) and its combination with dexamethasone (DEX).*

Materials and methods*: A unilateral model of hemorrhagic stroke was induced in 120 rats, which were divided into three groups: HS, HS+G-CSF, and HS+G-CSF+DEX. The control group consisted of sham-operated animals without stroke induction. On days 1, 3, 10, 30, and 60 post-injury, glial scar formation was assessed by immunohistochemistry. Brain sections were analyzed for GFAP expression and the presence of $CD44^+$, $CD68^+$, and $CD90^+$ cells. Densitometric analysis of the GFAP-positive area was performed.*

Results*. G-CSF increased the number of $CD44^+$ cells in the glial scar area during the acute phase after stroke. The combination of G-CSF and DEX attenuated the accumulation of $CD44^+$ cells but promoted their prolonged presence. G-CSF also enhanced the mobilization of $CD68^+$ cells to the site of hemorrhage, while DEX delayed their appearance, possibly due to its anti-inflammatory effects during the acute phase. $CD68^+$ cells in the lesion area may represent not only phagocytes but also mesenchymal progenitor cells. The mobilization of $CD90^+$ cells to the glial scar formation zone is limited and infrequent but increases under the influence of G-CSF. Nevertheless, their presence indicates the involvement of mesenchymal stem cells in regenerative processes following hemorrhagic stroke, as these cell types are not detected in the intact brain. Additionally, G-CSF reduced the intensity of astroglial activation following injury.*

Conclusions. *Cells of mesenchymal origin contribute to glial scar formation after hemorrhagic stroke, while such involvement is absent in the sham-operated group, aside from the rare appearance of $CD44^+$ cells. G-CSF modulates glial scar development by promoting the accumulation of mesenchymal cells in the injury area, which contributes to greater compactness of the scar without increasing its connective tissue component. G-CSF even reduces astrogliosis, a process that is otherwise exacerbated by dexamethasone during glial scar formation after brain hemorrhage.*

Keywords*: cerebral stroke; glial scar; mesenchymal stem cell; granulocyte colony-stimulating factor; CD44; CD68*

Mesenchymal stem cells (MSCs) are considered a potential tool for influencing regenerative processes in the injured nervous system, including stroke and peripheral nerve trauma. MSCs appear in affected organ areas, adhere through the expression of various adhesion molecules, secrete growth factors, and are likely to proliferate and differentiate into organ-specific cells [1].

The outcomes of administering allogeneic MSCs, derived from adipose stromal cells [2] and Wharton's jelly of the umbilical cord [3], have been highly anticipated. It is proposed that these cells tend to accumulate in the site of injury due to the expression of matrix-binding membrane receptors, such as CD40, leading to their accumulation and involvement in tissue regeneration [4]. However, this scenario depends on numerous factors, including systemic factors, such as the overall number of circulating MSCs and local factors, particularly the state of the tissue microenvironment, where inflammation plays a critical role in directing tissue regeneration.

The analysis of numerous studies on the brain following stroke has led to the formulation of a general cellular reaction scenario within the ischemic core and surrounding areas (penumbra or perihematomal region). Necrosis and the elimination of dead cells are associated with the formation of a glial scar, in which reactive astrocytes play a critical role. There is no definitive consensus on the source of the dynamic increase in the density of glial and non-glial cells at the boundary of the necrotic area, and the formation of the glial scar. It is suggested that these cells differentiate from MSCs, and the outcome of this process is highly dependent on the specific tissue microenvironment [5]. MSCs can be identified in the affected brain region through the expression of various cellular markers, based on their immunophenotypic characteristics. However, the exact differentiation pathway of MSCs in the brain following a stroke remains unclear.

Two non-mutually exclusive hypotheses have been proposed: the first suggests a direct differentiation of MSCs into organ-specific cells, while the second states that MSCs contribute to regeneration through the release of extracellular vesicles containing tissue growth factors, microRNAs, and other signalling molecules, thereby stimulating the repair of local cells via paracrine mechanisms [6,7,8]. Various growth factors play a crucial role in stimulating the accumulation, proliferation, and differentiation of MSCs. Well-known factors such as brain derived neurotrophic factor (BDNF), nerve growth factor (NGF), neurotensin (NTs), epidermal growth factor (EGF), and fibroblast growth factor (FGF) are secreted by different cells in the injured brain and contribute to the recovery of ischemic brain tissue damage. MSCs secrete BDNF, which promotes neurite elongation and axonal outgrowth [9]. Additionally, the combination of BDNF and NGF has been shown to effectively induce MSC differentiation into neurons, leading to the development of a neuronal morphological phenotype and the expression of neural markers [10].

Spontaneous and non-induced accumulation of CD44-expressing cells [11], which are potentially stem cells, has already been stated, although their ultimate fate in the brain remains poorly understood. These cells may differentiate into monocytes or dendritic cells [12]. The hypothesis of this study was to identify cells with a potential mesenchymal origin in the brain following stroke, and assess changes in their accumulation under the influence of granulocyte colony-stimulating factor (G-CSF). G-CSF is known to increase circulating levels of $CD31^+$, $CD34^+$, and $CD44^+$ cells in both healthy individuals and cancer patients. The study is also aimed to evaluate the effects of G-CSF in combination with dexamethasone (DEX) [13, 14]. It was hypothesized that G-CSF-induced expansion of the mesenchymal cell pool would facilitate their accumulation in the stroke-affected area, while DEX, due to its anti-inflammatory properties, might modulate their activity within the forming glial scar surrounding the hemorrhage.

The purpose: to identify cells in the glial scar of the brain following hemorrhagic stroke that may potentially have a mesenchymal origin, and assess changes in their quantity under the influence of G-CSF and its combination with dexamethasone.

Materials and methods

For the study we used adult (13-15 weeks) male Wistar rats (means body weight 205.6 ± 7.1 g), which were bred in the animal facilities of the Bogomolets National Medical University, Ukraine. All procedures involving laboratory animals were conducted in accordance with the EU Directive 2010/63/EU on the protection of animals used for scientific research, and the Bioethical Committee for Human and Animal Research at Bogomolets National Medical University (Ethics approval No. 160, dated 22/09/2022).

160 rats were divided into four groups, each consisting of 40 animals (8 rats per one term): sham-operated group (SH), hemorrhagic stroke group (HS), hemorrhagic stroke with G-CSF administration group (HS+G-CSF), and hemorrhagic stroke with combination therapy (HS+G-CSF+DEX). The animals were observed in 5 periods (days 1, 3, 10, 30 and 60 days after surgery). The sham-operated groups were used as a control for validation of stroke model.

The animals were under general anesthesia by thiopental (*Arterium*, Ukraine) 50 mg/kg intraperitoneally during the study procedures. We calculated the coordinates for autologous blood injection into the striatal and thalamic region with internal capsule using the stereotaxic atlas (L = 3.0-4.0; H = 4.0-6.0; AP = -1.0-3.0) [15].

We made an incision on the pre-shaved skin, produced a trepanation hole 1.0 mm in diameter, and injected 0.02 mL of autologous blood (without any coagulants, using a 1.0 mL frame-fixed syringe with needle G21). The needle was fixed and inserted into the brain, and the same amount of blood was re-injected after 10 minutes. The needle was then removed, and the wound was sutured with 2 USP polyamide filament, and irrigated with povidone-iodine solution Betadine (*Egis*, Hungary). Approximately 0.1 mL autologous blood was collected from the tail vein by syringe with needle G23. The mortality of animals ranged from 12 % to 33 % for each of the terms, and the average mortality was 22 %.

Recombinant human G-CSF (*Sanofi*, France) was administered as a single daily subcutaneous injection at a dose of 50 μg/kg, and dexamethasone (DEX) (*Lekhim*, Ukraine) was administered at a dose of 10 mg/kg on days 1, 2, and 3 of the study. Therefore, animals on day 1 and 2 got single and two doses of medicines.

The animals were euthanized by a lethal dose 250 mg/kg of thiopental (*Arterium*, Ukraine) intraperitoneally. The intracardial perfusion was performed using two solutions - the first one was 200 mL of physiological saline and the second 200 mL 4 % formaldehyde based on physiological saline at 4 ^{o}C. The brain was removed and placed in the last solution (pH 7.4), at 4 ^{o}C for 24 h). 3 mm thick sections were collected from each brain by making two frontal cuts (at the level of the needle insertion track). The brain samples were dehydrated in isopropanol and embedded in paraffin Surgipath Paraplast Regular (*Leica Biosystems*, Germany). Hematoxylin and eosin (H+E) staining was used to study the main structural violations. Immunohistochemical studies used 4 μm thick frontal brain sections following the manufacturer's antibody protocol. We used a rabbit monoclonal antibody for GFAP (cat no. MA5-12023, clone ASTRO6, *Invitrogen*, USA), a mouse monoclonal CD44 antibody (cat no. ab238464, clone OX49, *Abcam*, USA), a mouse CD68 monoclonal antibody (ab201340, clone C68/684, *Abcam*, USA) and mouse CD90/Thy1 monoclonal antibody (cat no. ab225, clone MRC OX-7, *Abcam*, USA) for immunohistochemical cell detection. All used antibodies were diluted at 1:200. The nuclei were stained with Gill's hematoxylin. The images of the reaction products were made using a diaminobenzidine-based detection system EnVision FLEX (*Dako*, Denmark). The brain slices with antibodies were incubated at 24 °C (with primary and secondary antibodies for 20 min and 10 min, respectively). Rat brain slices with some positive protein expressions were used as a positive control; for negative controls all procedures were

performed except for the use of primary antibodies. We examined preparations under BX51 microscope; their photos were taken with C3040ZOOM digital camera using DP-Soft 3.2 software (all – *Olympus*, Japan).

The density of GFAP in the formed glial scar was measured using the ImageJ 1.46 image analysis software ver. 1.8.0_172 (Wayne Rasband, NIH, USA) on microphotographs with a ×200 magnification (1280×960 RGB pixels, photoillumination mode, standardized exposure). We transformed the RGB photos into 8-bit images, and determined the threshold of immunopositive signals in the ROI. These regions were no longer than 200 μm from the hematoma or pseudocyst. 4-8 images per one brain section were analyzed. The analyzed data were represented as the percentage of the positive area in the total area of the ROI.

The quantity of $CD44^+$ and $CD68^+$ cells was assessed using the 3-point scale, where: 1 point (Low) = isolated cells; 2 points (Intermediate) = groups of cells around hemorrhage; 3 points (High) = multiple infiltrates within and around hemorrhage. This scoring system was chosen by analogy with density analysis of other mesenchymal cells [16]. The number of cells from 3 randomly selected regions (ROIs) per section of rat brain (3 fields per section × N samples) in the perihematomal region was averaged and expressed as cells per square millimeter [17]. The mean value obtained from the ROI of the sample was used for correlation analysis (regarding lesion volume, correlation of the appearance of cells expressing different CDs on the surface).

Statistical analysis of data was performed by unilateral ANOVA with the Bonferroni post hoc test and Mann-Whitney U test using StatPlus v. 7.0 software (*AnalystSoft Inc*., USA). Correlation analysis was conducted between the average case score of CD44 and CD68 measurements and the percentage of GFAP density, the differences among the groups were statistically significant at $p < 0.05$.

Results and discussion

In the SH group treks of the needle in rat brain were detected and local reactivity of astrocytes occurred. The thin layer or membrane formed by astrocytes, mainly their processes, surrounded the trek. Isolated cells or their small groups were detected in the lumen of trek. Active macrophages and $CD44^+$ cells were observed, but the last cell population was rarely detected on day 3. Therefore, we didn't evaluate their presence and only ascertained the fact of their detection.

In the ICH group around the perimeter of the brain hemorrhage, we observed the development of a glial scar, accompanied by the accumulation of cells with a blast-like phenotype. On day 1 hemorrhage was easily detected and no signs of astrocyte reactivity were observed around hematoma. By day 3, signs of scar formation were already evident, predominantly consisting of $GFAP^+$ cells, indicating the presence of reactive astrocytes (Fig. 1). Most of these cells exhibited a hypertrophied soma with short, thick, and sparsely branched processes, whereas in the contralateral hemisphere, they predominantly displayed a stellate morphology and, less frequently, a delicate spindle-shaped appearance.

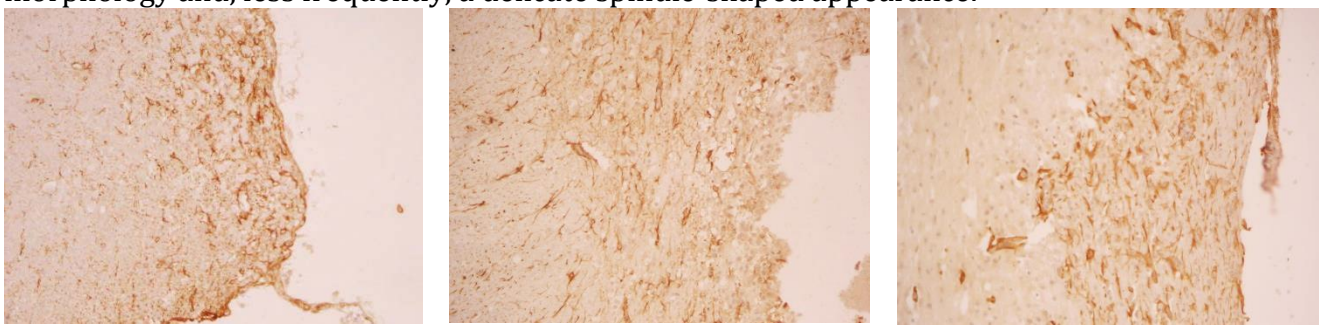

HS **HS+G-CSF** **HS+G-CSF+DEX**

Fig. 1. *Micrographs of rat brain sections on day 10 after HS modelling, immunohistochemical staining for GFAP (brown), light microscopy, ×200.*
Notes: HS – hemorrhagic stroke, HS+G-SCF – hemorrhagic stroke with G-CSF administration, HS+G-CSF+DEX – hemorrhagic stroke with G-CSF and dexamethasone.

The specific density of GFAP⁺ cells within the studied loci up to 100 μm showed an increasing trend until day 30, followed by a subsequent decline. In contrast, at a distance of 100-200 μm from the hematoma, the dynamics of glial scar development stabilized by day 10, with a lower density of GFAP expression detected thereafter (Fig. 2). In the HS+G-CSF group, a similar trend of decreasing GFAP⁺ cell density was observed, as in the HS group, although the difference between the groups was not statistically significant.

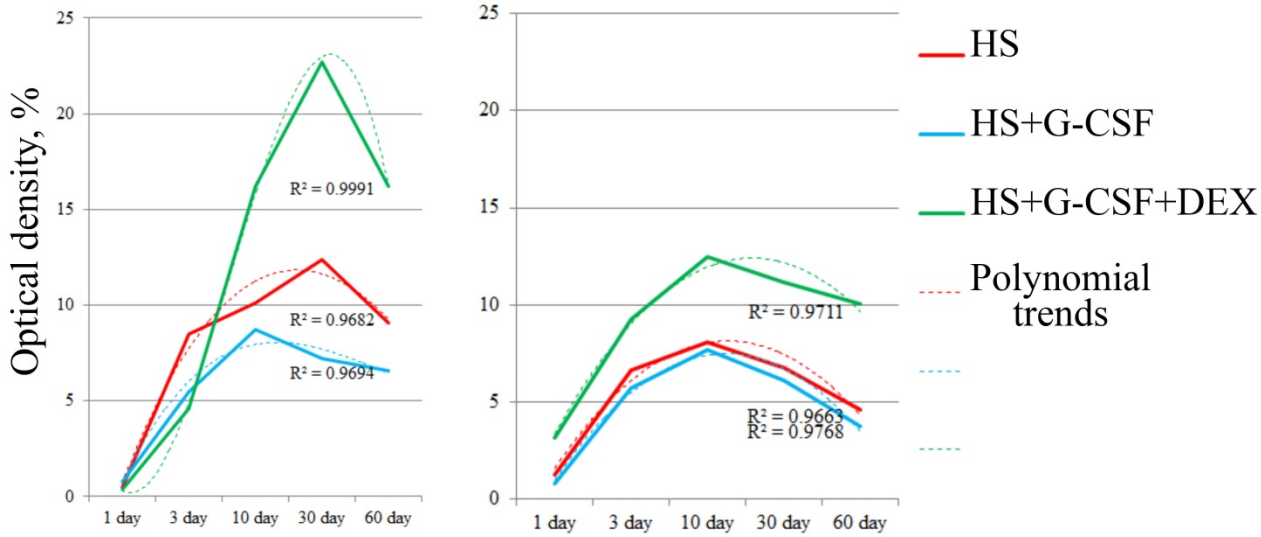

Fig. 2. *Densitometric assessment of the specific density of GFAP in the glial scar formation area after HS modelling. The left graph represents data within 100 μm, while the right graph shows data at a distance of 100-200 μm from the hemorrhage.*
Notes: HS – hemorrhagic stroke, HS+G-SCF – hemorrhagic stroke with G-CSF administration, HS+G-CSF+DEX – hemorrhagic stroke with G-CSF and dexamethasone.

Convincing evidence of increased astrocyte density was obtained in the HS+G-CSF+DEX group on day 30 compared to the HS and HS+G-CSF groups (ANOVA, $p < 0.05$). By day 60, the density of astrocytes had decreased, although the GFAP⁺ cells density remained higher. At this stage, the hemorrhage was eliminated, and a dense cellular network of GFAP⁺ cells was observed at the boundary of the pseudocyst.

The effect of DEX was reflected in a significant increase in astrocyte involvement in glial scar formation – nearly threefold within 100 μm and twofold within 200 μm (ANOVA, $p < 0.05$). In contrast, G-CSF partially reduced the reactive accumulation of astrocytes.

In the areas of glial scar formation, we observed the accumulation of blast-like cells, among which cells exhibited a positive membrane reaction for CD44 and a positive cytoplasmic reaction for CD68 and CD90 (Fig. 3). As early as day 1 after HS modelling, CD44⁺ cells were detected, with their number and accumulation foci visually increasing by day 3. However, by days 30 and 60, their quantity had decreased. In the HS+G-CSF group, both absolute and relative increases in the number of CD44⁺ cells were observed on days 1 and 3 compared to the HS group ($p < 0.05$, Mann-Whitney test).

Over time, the number of CD44⁺ cells decreased; however, on day 10, their levels remained significantly higher than in the HS group ($p < 0.05$, Mann-Whitney test). In the HS+G-CSF+DEX group, CD44+ cell accumulation was more intense during the first three days compared to the HS group, but lower than in the HS+G-CSF group. At the same time, the decline

in the number of these cells within the glial scar formation zone on day 30 was less pronounced than in the other two groups, and their levels remained elevated ($p < 0.05$, Mann-Whitney test). By day 60 of post-hemorrhage modelling, no statistically significant differences in $CD44^+$ cell content were observed between the experimental groups ($p > 0.05$).

Thus, the active local accumulation of $CD44^+$ cells into the hemorrhagic and glial scar formation areas occurred within the first 3-10 days, followed by their elimination after day 10. G-CSF enhanced this accumulation, while DEX prolonged their presence in the glial scar formation zone (Fig. 4).

CD68-expressing cells were primarily detected on day 10, appearing only sporadically in the HS group and in small focal clusters in the HS+G-CSF group ($p = 0.05$, Mann-Whitney test). Interestingly, in the HS+G-CSF+DEX group, these cells were rarely observed and detected only on days 30 and 60 (Fig. 4).

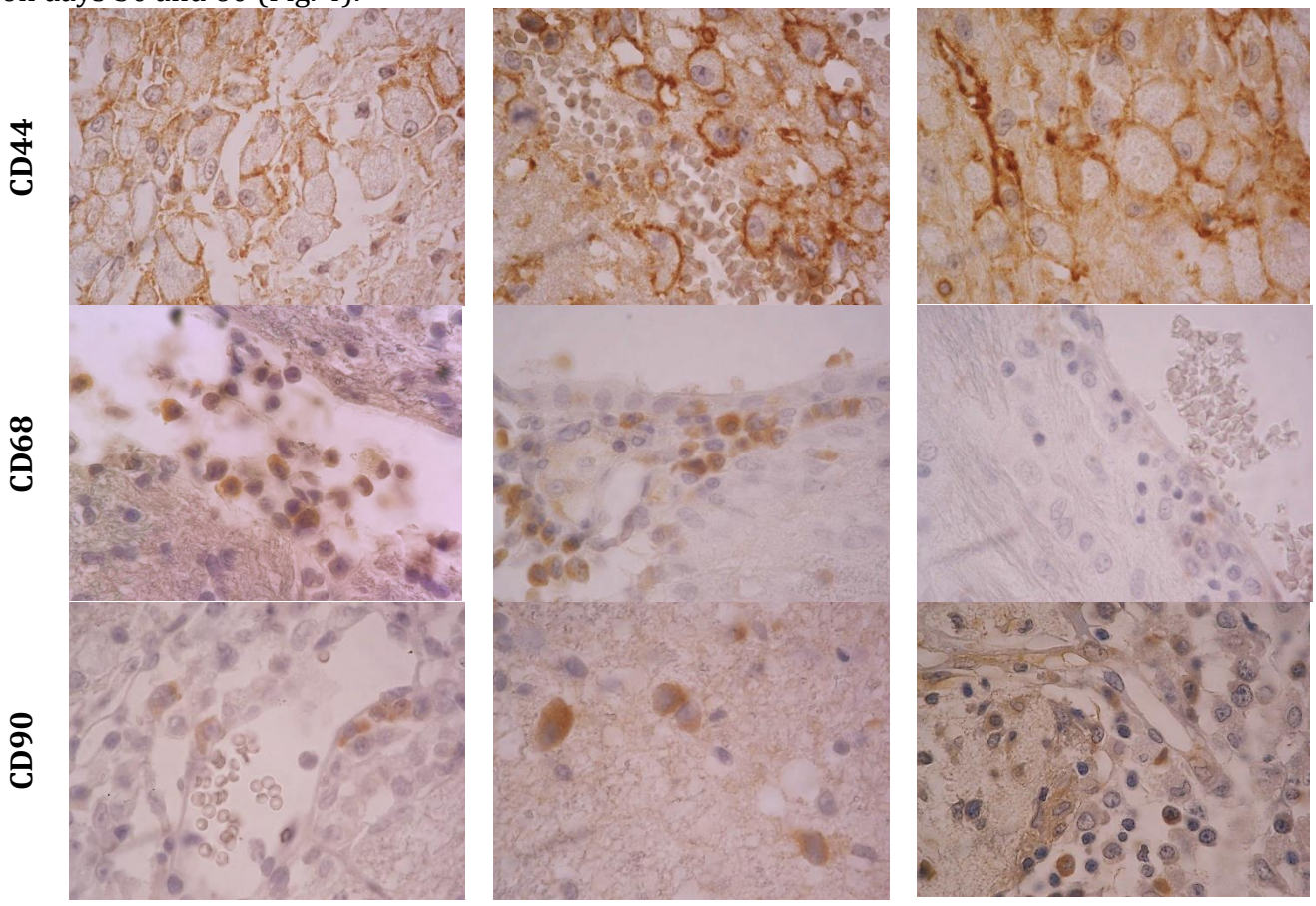

Fig. 3. *Micrographs of rat brain sections on day 10 after HS modelling, medial striatum, immunohistochemical staining for CD44, CD68, and CD90 (brown), light microscopy, ×1000.*
Notes: HS – hemorrhagic stroke, HS+G-SCF – hemorrhagic stroke with G-CSF administration, HS+G-CSF+DEX – hemorrhagic stroke with G-CSF and dexamethasone.

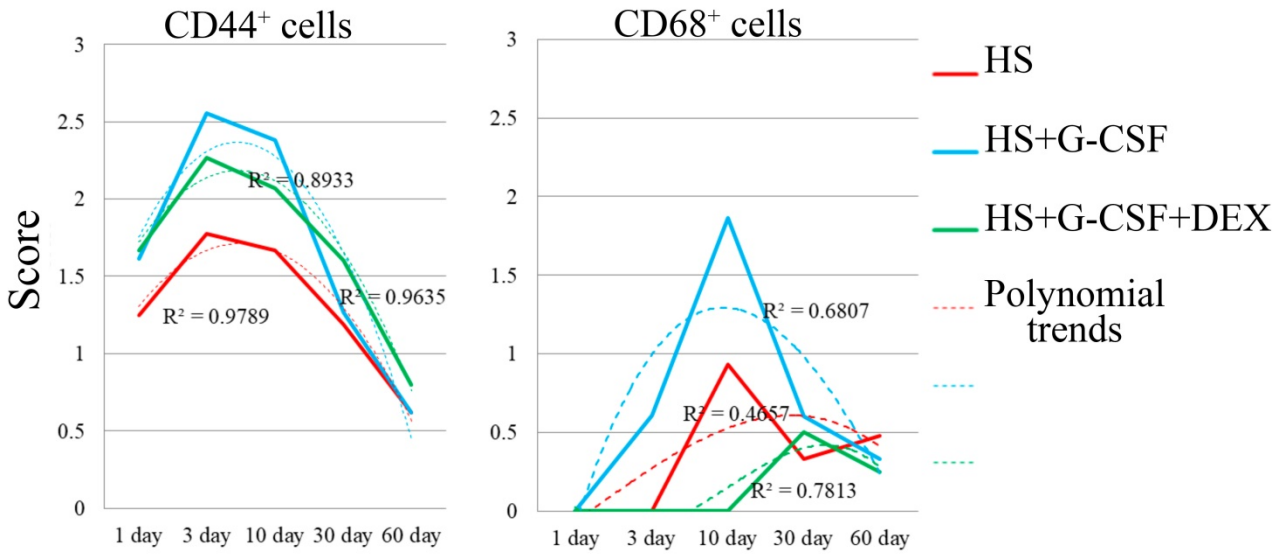

Fig. 4. *Accumulation of CD44⁺ and CD68⁺ cells after hemorrhagic stroke (HS) modelling.*
Notes: HS – hemorrhagic stroke, HS+G-SCF – hemorrhagic stroke with G-CSF administration, HS+G-CSF+DEX – hemorrhagic stroke with G-CSF and dexamethasone.

This suggests that G-CSF may have stimulated the appearance of CD68⁺ cells, whereas DEX delayed this process, likely due to its anti-inflammatory effects. The density of CD68⁺ cells in the glial scar areas was significantly lower compared to CD44⁺ cells. Although some differences were observed between groups, we did not identify any statistically significant differences ($p > 0.05$).

We detected only isolated CD90⁺ cells across all three experimental groups. The occurrence of these cells was relatively rare on days 3 and 10 after HS modelling (Fig. 3). Yet their presence is of significant importance, as it confirms the recruitment of mesenchymal stem cells into the perihematomal area following stroke.

We specifically emphasize this localization pattern, as CD90⁺ cells were not found directly within the glial scar formation loci, but rather within the lumens of newly formed blood vessels or at a certain distance from the hematoma, outside the glial scar regions. Although we did not obtain sufficient data to conclusively determine the involvement of CD90⁺ cells in glial scar formation, their presence strongly supports the participation of endogenous mesenchymal stem cells in compensatory and regenerative processes in the brain after HS. CD90⁺ cells were not detected in the intact and HS groups.

The findings of this study expand our understanding of cellular responses in the regions of scar formation following stroke, although many questions remain regarding the cellular sources contributing to glial scar formation. An increasing number of studies report the detection of CD44 on the surface of stem cells and in damaged tissues, which serve as niches for reparative regeneration involving progenitor cells [11]. Previous research has described the appearance and accumulation of CD44⁺ cells in the ischemic stroke core. While this phenomenon was limited to the acute phase of ischemia, the role of CD44⁺ cells in the injured brain and their involvement in glial scar formation remain unclear.

One of the early hypotheses suggested that CD44⁺ cells could be monocytes/macrophages participating in neuroinflammatory responses [18]. We partially agree with this hypothesis, as we also observed these cells during the acute phase of HS. Their accumulation was associated with the accelerated elimination of erythrocytic mass. However, these cells did not exhibit characteristics of phagocytosis of cellular debris or hemosiderin. Moreover, siderophages identified on days 30 and 60 post-hemorrhage did not express CD44, whereas some CD44⁺ cells continued to appear in glial scar formation sites.

For this reason, we support an alternative hypothesis that the accumulated blast-like $CD44^+$ cells originate from mesenchymal lineage and play a regenerative role in the damaged brain region. G-CSF is known to increase the content of $CD44^+$ stem cells in peripheral blood [19,20,21]. However, the differentiation outcomes of these cells remain unexplored, leaving unanswered questions regarding the tissue structures in which $CD44^+$ cells ultimately participate.

The detection of $CD44^+$ cells in areas of astrogliosis does not directly confirm their involvement in glial scar formation, nor does it allow us to assert that $CD44^+$ cells serve as a stem cell pool for astrocytic differentiation. However, it is intriguing that recent studies on the human brain have identified $CD44^+$ astrocytes in the hippocampus and cortex. Furthermore, protoplasmic astrocytes, which normally do not express CD44, have been shown to upregulate CD44 expression on their processes under hypoxic conditions [22]. Other researchers have considered CD44 as a marker for cerebellar astrocyte precursor cells [23,24]. CD44 expression is induced in vivo on glial cells in scar-forming regions surrounding inflammation [25]. However, there are also findings linking CD44 overexpression to the suppression of glial scar formation in the spinal cord [26].

The localization of CD44 does not fully overlap with CD68 expression [27]. We observed $CD68^+$ cells in the same regions as $CD44^+$ cells; however, differences in their morphology, particularly in cell size, suggest distinct immunophenotypic characteristics for these two populations. Moreover, the cellular identity of $CD68^+$ cells in the injured brain remains unclear. Macrophages, microglia, and stem cells are all known to express CD68, making it challenging to definitively classify these cells into a specific population.

Unlike active phagocytes, which are expected to accumulate in the stroke and inflammation areas to facilitate immune responses and phagocytosis, $CD68^+$ cells were rarely observed during the acute phase of stroke. Moreover, not all $CD68^+$ phagocytes express Iba1 [28]. This phenomenon is not exclusive to brain pathology following stroke. In a spinal cord injury model, $CD68^+$ cells, classified as part of the pro-inflammatory phenotype pool, were detected at the injury site after two weeks, and were eventually encapsulated by a dense glial scar [29]. While GFAP and Iba1 exhibited colocalization, CD68 and GFAP did not. Similarly, at three and four weeks, $CD68^+$ cells were found surrounded by $GFAP^+$ scar cells, with only a subpopulation of $Iba1^+$ cells co-expressing CD68.

These findings indicate that $CD68^+$ cells represent a heterogeneous population, encompassing both microglia and potentially mesenchymal stem cells, which do not appear to play a role in hemorrhage resolution or inflammation clearance. Consequently, the study of $CD68^+$ cells presents an even greater challenge compared to $CD44^+$ cells and requires further in-depth investigation to clarify their role and functional identity.

Similarly to $CD68^+$ cells, $CD90^+$ cells were also rare participants in glial scar formation. Moreover, we tend to believe that the presence of $CD90^+$ cells is not exclusively linked to glial scar formation, but may hypothetically be associated with various nonspecific regenerative processes in the brain. $CD90^+$ cells were more frequently detected in the G-CSF+DEX group. Given that DEX promoted their accumulation on days 30 and 60 [30], we hypothesize that DEX, by modulating inflammation, may have delayed the recruitment of mesenchymal cells or influenced their differentiation into a phenotypic population expressing CD90.

Our findings suggest that G-CSF in combination with DEX may enhance cellular responses in the glial scar region. However, the potential differentiation of mesenchymal cells into scar-forming astrocytes or other cell populations requires further investigation.

However, we are aware that our study has some limitations. We used antibodies for CD44, CD68 and CD90, while each of these is both a marker of mesenchymal cells and other populations, in particular differentiated cells. CD44 is also expressed on reactive astrocytes and immune cells, CD68 is a macrophage/microglia marker and CD90 is a more selective MSC marker but was rarely detected in this study, limiting its interpretability. Thus, each of these

CDs is a non-exclusive mesenchymal marker, For this reason, confocal multichannel microscopy would be a more sensitive method to determine the immunophenotypic profile of accumulating cells in brain hematome and glial scar. This work will be performed in more detail in the perspective of our study.

Conclusions

1. Mesenchymal-origin cells actively participate in the formation of the glial scar following brain hemorrhage, while penetrative brain injury in SH group does not cause recruiting these cells, excluding rare detection of $CD44^+$ cells.

2. G-CSF modulates glial scar formation in the brain after hemorrhagic stroke by enhancing the migration of mesenchymal cells into the perihematomous area. However, this does not lead to an increase in the connective tissue component of the glial scar; instead, it makes the scar more compact overall.

3. G-CSF even reduces astrogliosis, which is exacerbated by dexamethasone during glial scar formation around the brain hemorrhage.

Funding. *This study was funded by the Ministry of Health of Ukraine within the framework of project No. 0120U101376, titled "The study of restorative processes in the brain and nerve trunk during modulation of accumulation and differentiation of mesenchymal stem cells" (2023-2025).*

References

1. Cantore S, Crincoli V, Boccaccio A, Uva AE, Fiorentino M, Monno G, et al. Recent advances in endocrine, metabolic and immune disorders: mesenchymal stem cells (MSCs) and engineered scaffolds. Endocr Metab Immune Disord Drug Targets. 2018; 18(5):466-469. https://doi.org/10.2174/1871530318666180423102905
2. Panés J, García-Olmo D, Van Assche G, Colombel JF, Reinisch W, Baumgart DC, et al. ADMIRE CD Study Group Collaborators. Long-term efficacy and safety of stem cell therapy (Cx601) for complex perianal fistulas in patients with Crohn's disease. Gastroenterology. 2018; 154(5):1334-1342.e4. https://doi.org/10.1053/j.gastro.2017.12.020
3. Musialek P, Mazurek A, Jarocha D, Tekieli L, Szot W, Kostkiewicz M, et al. Myocardial regeneration strategy using Wharton's jelly mesenchymal stem cells as an off-the-shelf 'unlimited' therapeutic agent: results from the Acute Myocardial Infarction First-in-Man Study. Postepy Kardiol Interwencyjnej. 2015; 11(2):100-107. https://doi.org/10.5114/pwki.2015.52282
4. Liau LL, Ruszymah BHI, Ng MH, Law JX. Characteristics and clinical applications of Wharton's jelly-derived mesenchymal stromal cells. Curr Res Transl Med. 2020; 68(1):5-16. https://doi.org/10.1016/j.retram.2019.09.001
5. Liu J, Gao J, Liang Z, Gao C, Niu Q, Wu F, et al. Mesenchymal stem cells and their microenvironment. Stem Cell Res. Ther. 2022; 13(1):429. https://doi.org/10.1186/s13287-022-02985-y
6. La Greca A, Solari C, Furmento V, Lombardi A, Biani MC, et al. Extracellular vesicles from pluripotent stem cell-derived mesenchymal stem cells acquire a stromal modulatory proteomic pattern during differentiation. Exp. Mol. Med. 2018; 50(9):1-12. https://doi.org/10.1038/s12276-018-0142-x
7. Vonk LA, van Dooremalen SFJ, Liv N, Klumperman J, Coffer PJ, Saris DBF, et al. Mesenchymal stromal/stem cell-derived extracellular vesicles promote human cartilage regeneration in vitro. Theranostics. 2018; 8(4):906-920. https://doi.org/10.7150/thno.20746
8. Bobis-Wozowicz S, Kmiotek K, Kania K, Karnas E, Labedz-Maslowska A, Sekula M, et al. Diverse impact of xeno-free conditions on biological and regenerative properties of hUC-MSCs and their extracellular vesicles. J Mol Med. (Berl). 2017; 95(2):205-220. https://doi.org/10.1007/s00109-016-1471-7
9. Martins LF, Costa RO, Pedro JR, Aguiar P, Serra SC et al. Mesenchymal stem cells secretome-induced axonal outgrowth is mediated by BDNF. Sci Rep. 2017; 7:4153. https://doi.org/10.1038/s41598-017-03592-1
10. Choudhary P, Gupta A, Gupta SK, Dwivedi S, Singh S. Comparative evaluation of divergent concoction of NGF, BDNF, EGF, and FGF growth factor's role in enhancing neuronal differentiation of adipose-derived mesenchymal stem cells. Int J Biol Macromol. 2024; 260(2):129561. https://doi.org/10.1016/j.ijbiomac.2024.129561
11. Sawada R, Nakano-Doi A, Matsuyama T, Nakagomi N, Nakagomi T. CD44 expression in stem cells and niche microglia/macrophages following ischemic stroke. Stem Cell Investig. 2020; 7:4. https://doi.org/10.21037/sci.2020.02.02
12. Lee HJ, Jung H, Kim DK. IDO and CD40 May Be Key Molecules for Immunomodulatory Capacity of the Primed Tonsil-Derived Mesenchymal Stem Cells. Int J Mol Sci. 2021; 22(11):5772. https://doi.org/10.3390/ijms22115772
13. Lapierre V, Rossi JF, Heshmati F, Azar N, Vekhof A, Makowski C, et al. Ancestim (r-metHuSCF) plus filgrastim and/or chemotherapy for mobilization of blood progenitors in 513 poorly mobilizing cancer patients: the French compassionate experience. Bone Marrow Transplant. 2011; 46:936-942. https://doi.org/10.1038/bmt.2010.231
14. Lee S, Im SA, Yoo ES, Nam EM, Lee MA, Ahn JY, et al. Mobilization kinetics of CD34(+) cells in association with modulation of CD44 and CD31 expression during continuous intravenous

administration of G-CSF in normal donors. Stem Cells. 2000; 18(4):281-286. https://doi.org/10.1634/stemcells.18-4-281
15. Deng S, Feng S, Xin Y, He Y, Wang Y, Tian M, et al. Establishment of a rat model of severe spontaneous intracerebral hemorrhage. J Intensive Med. 2023; 4(1):108-117. https://doi.org/10.1016/j.jointm.2023.08.007
16. Gars E, Yousry SM, Babu D, Kurzer JH, George TI, Gratzinger D. A replicable CD271+ mesenchymal stromal cell density score: bringing the dysfunctional myelodysplastic syndrome niche to the diagnostic laboratory. Leuk Lymphoma. 2017; 58(7):1730-1732. https://doi.org/10.1080/10428194.2016.1251590
17. Choi BY, Kim OJ, Min SH, Jeong JH, Suh SW, Chung TN. Human Placenta-Derived Mesenchymal Stem Cells Reduce Mortality and Hematoma Size in a Rat Intracerebral Hemorrhage Model in an Acute Phase. Stem Cells Int. 2018; 2018:1658195. https://doi.org/10.1155/2018/1658195
18. Wang H, Zhan Y, Xu L, Feuerstein GZ, Wang X. Use of suppression subtractive hybridization for differential gene expression in stroke: discovery of CD44 gene expression and localization in permanent focal stroke in rats. Stroke. 2001; 32(4):1020-1027. https://doi.org/10.1161/01.str.32.4.1020
19. Chen Y, Rudolph KL. Granulocyte colony-stimulating factor acts on lymphoid-biased, short-term hematopoietic stem cells. Haematologica. 2021, 106(6):1516-1518. https://doi.org/10.3324/haematol.2020.271205
20. Christ O, Kronenwett R, Haas R, Zöller M. Combining G-CSF with a blockade of adhesion strongly improves the reconstitutive capacity of mobilized hematopoietic progenitor cells. Exp Hematol. 2001; 29(3):380-390. https://doi.org/10.1016/s0301-472x(00)00674-3
21. Mickiene G, Dalgėdienė I, Zvirblis G, Dapkunas Z, Plikusiene I, Buzavaite-Verteliene E, et al. Human granulocyte-colony stimulating factor (G-CSF)/stem cell factor (SCF) fusion proteins: design, characterization and activity. PeerJ. 2020; 8:9788. https://doi.org/10.7717/peerj.9788
22. Al-Dalahmah O, Sosunov AA, Sun Y, Liu Y, Madden N, Connolly E, et al. The Matrix Receptor CD44 Is Present in Astrocytes throughout the Human Central Nervous System and Accumulates in Hypoxia and Seizures. Cells. 2024; 13(2):129. https://doi.org/10.3390/cells13020129
23. Naruse M, Shibasaki K, Yokoyama S, Kurachi M, Ishizaki Y. Dynamic changes of CD44 expression from progenitors to subpopulations of astrocytes and neurons in developing cerebellum. PLoS One. 2013; 8(1):e53109. https://doi.org/10.1371/journal.pone.0053109
24. Cai N, Kurachi M, Shibasaki K, Okano-Uchida T, Ishizaki Y. CD44-positive cells are candidates for astrocyte precursor cells in developing mouse cerebellum. Cerebellum. 2012; 11(1):181-193. https://doi.org/10.1007/s12311-011-0294-x
25. Haegel H, Tölg C, Hofmann M, Ceredig R. Activated mouse astrocytes and T cells express similar CD44 variants. Role of CD44 in astrocyte/T cell binding. J Cell Biol. 1993; 122(5):1067-1077. https://doi.org/10.1083/jcb.122.5.1067
26. Guo J, Yang T, Zhang W, Yu K, Xu X, Li W, et al. Inhibition of CD44 suppresses the formation of fibrotic scar after spinal cord injury via the JAK2/STAT3 signaling pathway. iScience. 2024; 27(2):108935. https://doi.org/10.1016/j.isci.2024.108935
27. Luo W, Li Y, Zhao J, Niu R, Xiang C, Zhang M, et al. CD44-targeting hyaluronic acid-selenium nanoparticles boost functional recovery following spinal cord injury. J Nanobiotechnol. 2024; 22:37. https://doi.org/10.1186/s12951-024-02302-0
28. Sakuma R, Kawahara M, Nakano-Doi A, Takahashi A, Tanaka Y, Narita A, et al. Brain pericytes serve as microglia-generating multipotent vascular stem cells following ischemic stroke. J Neuroinflammation. 2016; 13(1):57. https://doi.org/10.1186/s12974-016-0523-9
29. Zhou ZL, Xie H, Tian XB, Xu H-L, Li W, Yao S, et al. Microglial depletion impairs glial scar formation and aggravates inflammation partly by inhibiting STAT3 phosphorylation in

astrocytes after spinal cord injury. Neural Regen Res. 2023; 18(6):1325-1331. https://doi.org/10.4103/1673-5374.357912
30. Graboviy OM, Mervinsky TS, Savosko SI, Yaremenko LM. Dynamics of changes in the representation of mesenchymal cells in the forming glial scar during dexamethasone application. Reports of Morphology. 2024; 30(3); 25-32. https://doi.org/10.31393/morphology-journal-2024-30(3)-03

The authors declare that there is no potential conflict of interest regarding the research, authorship and/or publication of this article.